

Distributed Fault Diagnosis for Multimachine Power Systems Based on Adaptive Approximation Approach

Shaoyan Wang¹, Tianrui Chen¹, and Guo Chen²

¹*the School of Automation, Guangdong University of Technology, Guangzhou, Guangdong China*

²*the School of Electrical Engineering and Telecommunications, University of New South Wales, Sydney, NSW 2052, Australia*

Abstract—This paper presents a distributed fault diagnosis architecture for multimachine power system, which is considered as a set of subsystems with interacted dynamic. In the distributed framework, a local fault diagnosis component is designed for each subsystem, responsible for both fault detection and isolation. A fault caused by unexpected admittance changes is detected by applying analytical redundancy relations of residuals of approximator-based estimators and corresponding adaptive thresholds. The fault isolation mechanism is conducted through a set of dedicated estimators. In addition, to analyze the performance of proposed fault diagnosis scheme, fault detectability and isolability are given. Simulation results for IEEE 9-bus and IEEE 39-bus system are presented to prove the effectiveness of the proposed distributed fault diagnosis method.

Index Terms—PMU, distributed system, fault detection, fault isolation, multi-machine power system

I. INTRODUCTION

Power systems are critical infrastructures in modern society, whose stability and safety rely on an effective fault diagnosis and tolerance system [1]. Over the past decades, there have been a large amount of research activities in designing a fault diagnosis scheme for power system. From the perspective of system fault diagnosis, these fruits can be categorized into model-based methods [2]–[8], signal-based methods [9]–[14] and knowledge-based methods [15]–[21]. Knowledge-based approaches, applying particular artificial intelligent tools to accessible historic process data (thus also refers to data-driven methods), stand for the mainstream to build an integrated fault diagnosis scheme. The majority of the data-driven methods are based on information gathered from the conventional Supervisory Control And Data Acquisition (SCADA) system, including the condition of protective relays and circuit breakers, three phase voltage and current signal [15]–[17]. While model-based methods, especially the classic observer-based and estimator-based method, have less practical cases, which mainly ascribes to the low refresh rate of the SCADA system. Limited to low sampling frequency, only the static model of power system can be used, implying that over-constrained operations are necessary to ensure safety and reliability [22].

In the last two decades, the emerging synchronous Phasor Measurement Units (PMU) with a higher sampling frequency have been widely applied, providing new source of data for

power systems. PMU provides real-time state monitoring with low latency and high refresh rate, breaking the ground to model-based fault diagnosis methods in consideration of power system's dynamic model, which is described by the so-called swing equation [22]. Such equation describes how do multiple generators interconnect and influence each other in phase angle and speed.

Related studies mainly rely on the monitoring of system states and apply some online schemes, in consideration of actuator fault such as abnormal generator output [4], [22], admittance change caused by topology attack [2], [3], [5], or sensor fault [6]. In [22], the linear-structure Unknown Input Observer (UIO) is designed and applied to the linearized power system dynamic model. In [4], the adaptive threshold is derived by analyzing a designed Lyapunov function. In [3], the author transfers the fault diagnosis problem into a compressive sensing problem, which is calculated through a sparse Bayesian formulation. In [6], significant traits of the proposed fault detection and isolation scheme such as fault detectability, fault isolability, stability and learning capability are analyzed. In [5], by reducing appropriate neurons, a downsizing RBF neural network is used to approximate the interconnected dynamic and to make a fast fault diagnosis.

Since the swing equation reflects the inherent physically decentralized nature of power system, a distributed fault diagnosis mechanism is more appropriate to apply. Compared with centralized methods, distributed methods ask for less computing resources and lower requirements for measurement and communication, thus have aroused public interest and gradually become a main solution in dealing with network system [2]. A typical distributed fault diagnosis structure consists of several intelligent agents, which can carry out fault diagnosis reasoning individually [23]. Such intelligent agents are mainly constructed with information of local measurements, local observers, limitation factors and subsystem models obtained by decomposition methods [24]. Limit checking is widely used for making fault-detection and fault-isolation decisions. In order to construct a robust residual or fault indicator against modeling errors and process disturbance, some researchers integrated adaptive approximator into the traditional nonlinear observer, and testified in some industrial occasions such as heating, ventilation and air-conditioning

(HVAV) system, multi-tank system, and robot manipulators [23], [25], [26]. In these studies, three main focuses are analyzed: derivation of adaptive threshold, investigation of fault detectability and isolability, and investigation of estimator's stability and learning ability.

In this paper, we consider a three-phase short circuit fault which directly causes a topology change, and apply a distributed fault diagnosis scheme that encompasses multiple diagnosis agents. Approximator with adaptive parameters is used to approximate the interconnection terms in the dynamic model of the power system, with limited phasor information of adjacent generators. The approximator can adjust the admittance parameters in the interconnection term and compensate for the effects of parameter modeling errors. Based on the dynamic model of each generator, a corresponding fault diagnosis component is established. Each diagnosis component completes independent fault detection and location tasks, through a series of estimators with approximators: in fault detection, a fault detection and approximation estimator (FDAE) and corresponding threshold are designed; in fault isolation, a series of fault isolation estimators (FIE) which correspond to different defined fault events and corresponding thresholds are designed. Each threshold is decoupled from its corresponding fault event, so as to locate the fault. In addition, this paper also analyzes the fault detectability and isolability problem under this scheme. Finally, the scheme is simulated in IEEE 9 and 39 bus systems to verify its effectiveness and reliability.

The paper is organized as follows: In section II, the discrete model of generator dynamic is established. In section III, the adaptive thresholds for FDAE and FIE are derived and the detectability and isolability are given. In section IV, simulation results for IEEE 9-bus and 39-bus systems are presented. Finally, the conclusion remarks are drawn in section V.

II. PROBLEM FORMULATION

A. Description of Multimachine Power System

Consider a general multimachine power system, which is composed of N buses and transmission lines connecting the buses. Applying concepts in graph theory, the structure of the power system is described by $\Sigma : \mathcal{G}(\mathcal{V}, \mathcal{E})$, where $\mathcal{V} = \{1, \dots, N\}$ is the node set corresponding to the bus indices, $\mathcal{E} \triangleq \{(i, j) : i, j \in \mathcal{V}\}$ is the edge set in which node i and j share a connecting line. The generator set is $\mathcal{V}_g = \{n_1, \dots, n_g\}_{1 \times N_g}$, while $\mathcal{V}_g \subset \mathcal{V}$. Applying *Kron Reduction*, nodes other than generator nodes can be simplified and a compressed admittance matrix is obtained [27]. Neglecting those weakly connected dynamic, a simplified edge set $\mathcal{E}_g \triangleq \{(i, j) : i, j \in \mathcal{V}_g\}$ is obtained, while for each generator bus i , the interconnection set $\mathcal{N}_i \triangleq \{j \in \mathcal{V}_g | (i, j) \in \mathcal{E}_g\}$ is introduced. Generator i together with generators $j \in \mathcal{N}_i$ constitute the i th subsystem, that is

Definition 1. The structure of subsystem i is $\Sigma_i : \mathcal{G}(\mathcal{V}_i, \mathcal{E}_i)$, where $\mathcal{V}_i = \{i\} \cup \mathcal{N}_i$, $\mathcal{E}_i = \{(i, j) : (i, j) \in \mathcal{E}_g, j \in \mathcal{N}_i\}$.

Remark. The simplified subsystem is constructed in the premise of adequate detecting and isolating capability. Under

this precondition, the connecting complexity is reduced and the real-time is improved.

For each $i \in \mathcal{V}_g$, the dynamic of the generator bus i is described by the nonlinear *swing function* [28]

$$\begin{aligned} \dot{\delta}_i(t) &= \omega_i(t) \\ \dot{\omega}_i(t) &= -\frac{d_i}{m_i}\omega_i(t) + \frac{1}{m_i}P_{mi}(t) - \frac{1}{m_i} \sum_{j \in \mathcal{N}_i} P_{ij}(t) \\ &\quad + \beta(t - T_0) \frac{1}{m_i} \sum_{j \in \mathcal{N}_i} \Delta P_{ij}^s(t) + \eta_i(\delta_i, \omega_i, P_{mi}, t) \end{aligned} \quad (1)$$

where δ_i is the phase angle of node i , ω_i is the relative speed of the of node i , m_i and d_i are the inertia and damping coefficients of the machines, respectively. P_{mi} is the mechanical input power, P_{ij} is the active power flow between machine i and j . $\eta_i(\delta_i, \omega_i, P_{mi}, t)$ is unstructured local modeling uncertainty reflecting multiple sources of uncertainty, such as discretization error, uncertainty in modelling parameters, system disturbances and so on.

Assumption 1. No power losses nor ground admittances are considered in transmission lines, which states that the active power flow between buses is completely determined by the voltage, phase of buses, and the admittance between buses, that is [3]

$$P_{ij}(t) = |E_i||E_j|G_{ij} \cos \delta_{ij}(t) + |E_i||E_j|B_{ij} \sin \delta_{ij}(t) \quad (2)$$

where $\mathbf{E}_i = |E_i|e^{i\delta_i}$ denote the complex voltage of node i with imaginary unit \mathbf{i} , $\delta_{ij}(t) := \delta_i(t) - \delta_j(t)$ is the phase angle difference between node i and j , G_{ij} and B_{ij} is the branch conductance and susceptance between node i and j respectively.

$\beta(t - T_0)$ is a step function representing the time profile of fault, which occurs at some unknown time T_0 . The occurrence of fault in transmission lines results in the change of branch conductance and susceptance between buses, so as the active power flow, that is

$$\begin{aligned} \Delta P_{ij}^s(t) &= |E_i||E_j|(G_{ij} - G_{ij}^s) \cos \delta_{ij}(t) \\ &\quad + |E_i||E_j|(B_{ij} - B_{ij}^s) \sin \delta_{ij}(t) \end{aligned} \quad (3)$$

where G_{ij}^s and B_{ij}^s are the branch conductance and susceptance between node i and j respectively, after the occurrence of fault s .

B. Model Discretization

The mechanical input power P_{mi} can be regarded as constant during sampling intervals $[t_k, t_{k+1}]$. Applying the forward Euler discretization method to (1) with sampling period τ , via replacing $\dot{\delta}_i$ and $\dot{\omega}_i$ by $\frac{\delta_i(t_{k+1}) - \delta_i(t_k)}{\tau}$ and $\frac{\omega_i(t_{k+1}) - \omega_i(t_k)}{\tau}$, we obtain

$$\begin{aligned} \delta_i(k+1) &= \delta_i(k) + \tau \omega_i(k) \\ \omega_i(k+1) &= (1 - \frac{d_i \tau}{m_i}) \omega_i(k) + \frac{\tau}{m_i} P_{mi}(k) + g_i(\delta_i(k), z_i(k)) \\ &\quad + \beta(k\tau - T_{i0}) \phi_i(\delta_i(k), z_i(k)) \\ &\quad + \eta_i(\delta_i(k), \omega_i(k), P_{mi}(k), k) \end{aligned} \quad (4)$$

where

$$\begin{aligned} g_i(\delta_i(k), z_i(k)) &= -\frac{\tau}{m_i} \sum_{j \in \mathcal{N}_i} P_{ij}(k) \\ \phi_i(\delta_i(k), z_i(k)) &= \frac{\tau}{m_i} \sum_{j \in \mathcal{N}_i} \Delta P_{ij}^s(k) \end{aligned} \quad (5)$$

with notation $k := k\tau$

Remark. While the data refreshing cycle of the traditional SCADA system is around 4s, PMU can provide a sampling period τ as short as 4×10^{-5} s [3], ensuring the approximation of $\dot{\delta}_i$ and $\dot{\omega}_i$ by Euler forward discretisation adequately precise.

Assumption 2. The system state ω_i remains bounded before and after the occurrence of a fault. That is, there exist a stable region \mathcal{R}_i^ω , such that $\omega_i(t) \in \mathcal{R}_i^\omega, \forall t \geq 0$. This boundary condition is obtained by using governors equipped on generators with feedback control [29]

$$\dot{P}_{mi} = (P_{refi} - P_{mi} - \Delta\omega_i/R_i) / T_{gi} \quad (6)$$

where R_i is the speed regulation factor of the generator i . T_{gi} is the total time constant of the governor and turbine. $\Delta\omega_i = \omega_i - \omega_R$, where $\omega_R = 120\pi$ is the reference speed. This means that if a disturbance or fault happens, generators will adjust their mechanical input to pull system state back into a steady area.

Assumption 3. The unstructured model uncertainty $\eta_i(\delta_i, \omega_i, P_{mi}, k)$ is unknown but bounded by a known function

$$|\eta_i(\delta_i, \omega_i, P_{mi}, k)| \leq \bar{\eta}_i(\delta_i, \omega_i, P_{mi}, k) \quad (7)$$

III. DISTRIBUTED FAULT DETECTION AND ISOLATION

The distributed fault diagnosis scheme is composed of N_g diagnosis agents. Each diagnosis agent i ($i \in \mathcal{N}_g$) is designed based on the dynamic model of subsystem Σ_i in (4). Specifically, each diagnosis agent consists of a *fault detection and approximation estimator* (FDAE) and a group of *fault isolation estimators* (FIEs). The fault detection and isolation logic relies on limit-checking between the state estimation error and corresponding thresholds. In healthy condition, only FDAE is operating to monitor the subsystem and approximate the unknown branch conductance and susceptance between buses. If a fault is detected, the group of FIEs will be activated to monitor the current system and generate isolation announcements.

A. Distributed Fault Detection Scheme

Based on the discrete-time model of subsystem Σ_i in (4), the FDAE is designed as:

$$\begin{aligned} \hat{\delta}_i(k+1) &= \hat{\delta}_i(k) + \tau \hat{\omega}_i(k) \\ \hat{\omega}_i(k+1) &= (1 - \frac{d_i \tau}{m_i}) \hat{\omega}_i(k) + \frac{\tau}{m_i} P_{mi}(k) + \hat{g}_i(\delta_i(k), z_i(k); \hat{\theta}_i) \\ &\quad + \lambda_i(\hat{\omega}_i(k) - \omega_i(k)) \end{aligned} \quad (8)$$

where $0 < \lambda_i < 1$ is a design constant to adjust estimation degree, $\hat{\omega}_i$ is the estimate of state ω_i , $\hat{g}_i(\delta_i, z_i; \hat{\theta}_i)$ is an

online approximation model designed to learn the unknown interconnection function $g_i(\delta_i, z_i)$, while $\hat{\theta}_i$ is a vector of adjustable parameters:

$$\begin{aligned} \hat{g}_i(\delta_i(k), z_i(k); \hat{\theta}_i) &:= -\frac{\tau}{m_i} \sum_{j \in \mathcal{N}_i} |E_i| |E_j| \hat{G}_{ij} \cos \delta_{ij}(k) \\ &\quad + |E_i| |E_j| \hat{B}_{ij} \sin \delta_{ij}(k) \\ \hat{\theta}_i &:= (\hat{G}_{ij}, \hat{B}_{ij})^T \\ \hat{G}_{ij} &= \text{col}(\hat{G}_{ij}, j \in \mathcal{N}_i) \\ \hat{B}_{ij} &= \text{col}(\hat{B}_{ij}, j \in \mathcal{N}_i) \end{aligned} \quad (9)$$

Applying adaptive parameter estimation techniques, with the following adaptive law [30]:

$$\hat{\theta}_i(k+1) = \mathcal{P}(\hat{\theta}_i(k) + \gamma_i(k) H_i^T(k) \sigma_i(k+1)) \quad (10)$$

where $\sigma_i(k+1) = \epsilon_i(k+1) - \lambda_i \epsilon_i(k)$ is the filtered speed estimation error, $\epsilon_i(k) := \hat{\omega}_i(k) - \omega_i(k)$ is the speed estimation error, $\gamma_i(k) \triangleq \mu_i / (\varepsilon_i + \|H_i^T(k)\|_F^2)$ is the learning rate, $\|\cdot\|_F$ denotes the Frobenius norm, ε_i and μ_i are design constants with $\varepsilon_i > 0$, $0 < \mu_i < 2$ that guarantee the stability of the learning law. H_i is a matrix representing the gradient of the on-line approximator $\hat{g}_i(\delta_i(k), z_i(k); \hat{\theta}_i)$ with respect to its adjustable parameters,

$$H_i \triangleq \left[\frac{\partial \hat{g}_i(\delta_i, z_i; \hat{\theta}_i)}{\partial \hat{\theta}_i} \right] \quad (11)$$

\mathcal{P} is a projection operator that restricts $\hat{\theta}_i$ to a pre-defined compact and convex set $\hat{\Theta}_i$, that is

$$\mathcal{P}(\hat{\theta}_i) \triangleq \begin{cases} \hat{\theta}_i, & \text{if } |\hat{\theta}_i| \leq M_{\hat{\Theta}_i} \\ \frac{M_{\hat{\Theta}_i} \hat{\theta}_i}{|\hat{\theta}_i|}, & \text{if } |\hat{\theta}_i| > M_{\hat{\Theta}_i} \end{cases} \quad (12)$$

In general, allowing the online approximator \hat{g}_i to match the unknown function g_i perfectly is a difficult task, which requires persistence of excitation condition (PE condition). Let $\hat{\theta}_i^*$ denotes the optimal parameter estimate that minimizes the difference between \hat{g}_i and g_i within the compact convex set $\hat{\Theta}_i$, that is

$$\begin{aligned} \hat{\theta}_i^* &\triangleq \arg \min_{\hat{\theta}_i \in \hat{\Theta}_i} \max_{\mathcal{R}} \left\| -\frac{\tau}{m_i} \sum_{j \in \mathcal{N}_i} |E_i| |E_j| (G_{ij} - \hat{G}_{ij}) \cos \delta_{ij} \right. \\ &\quad \left. + |E_i| |E_j| (B_{ij} - \hat{B}_{ij}) \sin \delta_{ij} \right\| \end{aligned} \quad (13)$$

Noticing that the structure of \hat{g}_i is linearly parameterized, so as the optimal approximating bias, we obtain $\hat{g}_i(\delta_i(k), z_i(k); \hat{\theta}_i) - \hat{g}_i(\delta_i(k), z_i(k); \hat{\theta}_i^*) = H_i^T(k) \tilde{\theta}_i(k)$, where $\tilde{\theta}_i := \hat{\theta}_i - \hat{\theta}_i^*$ denotes the parameter estimation error.

In healthy condition, the state estimate error $\epsilon_i(k) \triangleq \hat{\omega}_i(k) - \omega_i(k)$ is given by

$$\begin{aligned} \epsilon_i(k+1) &= (1 - \frac{d_i \tau}{m_i} + \lambda_i) \epsilon_i(k) + H_i^T(k) \tilde{\theta}_i(k) \\ &\quad - \tau \eta_i(\delta_i(k), \omega_i(k), P_{mi}(k), k) \\ &\quad - \frac{\tau}{m_i} \sum_{j \in \mathcal{N}_i} |E_i| |E_j| ((\hat{G}_{ij}^* - G_{ij}) \cos \delta_{ij}(k) \\ &\quad + (\hat{B}_{ij}^* - B_{ij}) \sin \delta_{ij}(k)) \end{aligned} \quad (14)$$

The solution of the above difference equation is:

$$\begin{aligned} \epsilon_i(k) = & \sum_{h=0}^{k-1} \left(1 - \frac{d_i \tau}{m_i} + \lambda_i \right)^{k-1-h} \left(H_i^T(h) \tilde{\theta}_i(h) \right. \\ & - \tau \eta_i(\delta_i(h), \omega_i(h), P_{mi}(h), h) \\ & - \frac{\tau}{m_i} \sum_{j \in \mathcal{N}_i} |E_i| |E_j| ((\hat{G}_{ij}^* - G_{ij}) \cos \delta_{ij}(h) \\ & \left. + (\hat{B}_{ij}^* - B_{ij}) \sin \delta_{ij}(h)) \right) + \left(1 - \frac{d_i \tau}{m_i} + \lambda_i \right)^k \epsilon_i(0) \end{aligned} \quad (15)$$

By applying the triangular inequality, we have

$$\begin{aligned} |\epsilon_i(k)| \leq & \sum_{h=0}^{k-1} \left(1 - \frac{d_i \tau}{m_i} + \lambda_i \right)^{k-1-h} \left(\|H_i^T(h)\| \kappa_i(h) \right. \\ & + \tau \eta_i(\delta_i(h), \omega_i(h), P_{mi}(h), h) \\ & + \left| \frac{\tau}{m_i} \sum_{j \in \mathcal{N}_i} |E_i| |E_j| ((\hat{G}_{ij}^* - G_{ij}) \cos \delta_{ij}(h) \right. \\ & \left. + (\hat{B}_{ij}^* - B_{ij}) \sin \delta_{ij}(h)) \right| \Bigg) + \left(1 - \frac{d_i \tau}{m_i} + \lambda_i \right)^k |\epsilon_i(0)| \end{aligned} \quad (16)$$

The estimate $\hat{\theta}_i$ belongs to a known compact set Θ_i . So that for a suitable κ_i dependent on the geometric properties of the set Θ_i , exists $\|\hat{\theta}_i\| \leq \kappa_i$. Moreover,

$$\begin{aligned} & \left| \frac{\tau}{m_i} \sum_{j \in \mathcal{N}_i} |E_i| |E_j| ((\hat{G}_{ij}^* - G_{ij}) \cos \delta_{ij}(h) \right. \\ & \quad \left. + (\hat{B}_{ij}^* - B_{ij}) \sin \delta_{ij}(h)) \right| \leq \\ & \quad K_{\hat{g}} \|col(\delta_i(h), z_i(h))\| \\ & + \left| \frac{\tau}{m_i} \sum_{j \in \mathcal{N}_i} |E_i| |E_j| (G_{ij} \cos \delta_{ij}(h) + B_{ij} \sin \delta_{ij}(h)) \right| \end{aligned} \quad (17)$$

where $K_{\hat{g}_i}$ denotes the Lipschitz constant of the adaptive approximator on a known compact set. Combining (16) and (17), we have

$$\begin{aligned} |\epsilon_i(k)| \leq & \sum_{h=0}^{k-1} \left(1 - \frac{d_i \tau}{m_i} + \lambda_i \right)^{k-1-h} \left(\|H_i^T(h)\| \kappa_i(h) \right. \\ & + \tau \eta_i(\delta_i(h), \omega_i(h), P_{mi}(h), h) \\ & + K_{\hat{g}} \|col(\delta_i(h), z_i(h))\| \\ & + \left| \frac{\tau}{m_i} \sum_{j \in \mathcal{N}_i} |E_i| |E_j| (G_{ij} \cos \delta_{ij}(h) + B_{ij} \sin \delta_{ij}(h)) \right| \Bigg) \\ & + \left(1 - \frac{d_i \tau}{m_i} + \lambda_i \right)^k |\epsilon_i(0)| \triangleq \bar{\epsilon}_i(k) \end{aligned} \quad (18)$$

where $\bar{\epsilon}_i(k)$ is the designed adaptive threshold for fault detection, so that under healthy condition, $|\epsilon_i(k)| \leq \bar{\epsilon}_i(k)$ is satisfied. The following fault detection logic is given.

Proposition 1 (Local Fault Detection Logic). The detection decision on the occurrence of a fault in the i th subsystem is made, when there exist a time t , such that $|\epsilon_i(t)| > \bar{\epsilon}_i(t)$. The fault detection time $T_{id} = \tau K_{id}$ is defined as the first time

instant such that $|\epsilon_i(K_{id})| > \bar{\epsilon}_i(K_{id})$, for some $T_d \geq T_0$, that is

$$T_d \triangleq \inf_{i=1}^N \bigcup_{t=0}^{\infty} \{t \geq 0 : |\epsilon_i(t_k)| > \bar{\epsilon}_i(t_k)\} \quad (19)$$

It's worth to mention that condition $|\epsilon_i(k)| \leq \bar{\epsilon}_i(k)$ is a sufficient unnecessary condition for proposition "the system is healthy", which means that no fault function has appeared in system dynamic. However, there are still some kinds of faults sufficiently small to detect. Hence, an analysis on the fault detectable condition is given.

B. Fault Detectability Analysis

We consider the case that, a fault s occurs at some unknown time $T_0 > 0$ and is eventually detected by the i th diagnosis component at some known time instant $T_d \geq T_0$. Therefore, for $T_0 \leq t \leq T_d$ the on-line approximator is learning some new unknown parameters G_{ij}^s and B_{ij}^s . In this respect, we rewrite definition (13) to take into account for the occurred fault, that is

$$\begin{aligned} \hat{\theta}_i^{*s} \triangleq & \arg \min_{\theta_i \in \Theta_i} \max_{\mathcal{R}} \left\| -\frac{\tau}{m_i} \sum_{j \in \mathcal{N}_i} |E_i| |E_j| (G_{ij}^s - \hat{G}_{ij}) \cos \delta_{ij} \right. \\ & \left. + |E_i| |E_j| (B_{ij}^s - \hat{B}_{ij}) \sin \delta_{ij} \right\| \end{aligned} \quad (20)$$

For $t > T_0$, the state estimate error becomes:

$$\begin{aligned} \epsilon_i(k) = & \sum_{h=0}^{k-1} \left(1 - \frac{d_i \tau}{m_i} + \lambda_i \right)^{k-1-h} \left(H_i^T(h) \tilde{\theta}_i^f(h) \right. \\ & - \tau \eta_i(\delta_i(h), \omega_i(h), P_{mi}(h), h) \\ & - \frac{\tau}{m_i} \sum_{j \in \mathcal{N}_i} |E_i| |E_j| ((\hat{G}_{ij}^{*s} - G_{ij}^s) \cos \delta_{ij}(h) \\ & \left. + (\hat{B}_{ij}^{*s} - B_{ij}^s) \sin \delta_{ij}(h)) \right) + \left(1 - \frac{d_i \tau}{m_i} + \lambda_i \right)^k \epsilon_i(0) \end{aligned} \quad (21)$$

where $\tilde{\theta}_i^f := \hat{\theta}_i - \hat{\theta}_i^{*s}$. To build a connection between the estimation error between healthy and faulty condition, we introduce *mismatch function*:

$$\chi_i(k) \triangleq -\frac{\tau}{m_i} \sum_{j \in \mathcal{N}_i} |E_i| |E_j| (\Delta G_{ij}^s \cos \delta_{ij}(k) + \Delta B_{ij}^s \sin \delta_{ij}(k)) \quad (22)$$

where $\Delta G_{ij}^s = G_{ij} - G_{ij}^s$, $\Delta B_{ij}^s = B_{ij} - B_{ij}^s$ are actual parameter bias, that is $\Delta \theta_i^s := (\Delta G_{ij}^s, \Delta B_{ij}^s)$.

So that the state estimate error at the occurrence of fault ($t > T_0$) can be written as

$$\begin{aligned} \epsilon_i(k) = & \sum_{h=0}^{k-1} \left(1 - \frac{d_i \tau}{m_i} + \lambda_i \right)^{k-1-h} \left(H_i^T(h) \tilde{\theta}_i(h) \right. \\ & - \tau \eta_i(\delta_i(h), \omega_i(h), P_{mi}(h), h) + \chi_i(\delta_i(h), z_i(h)) \\ & - \frac{\tau}{m_i} \sum_{j \in \mathcal{N}_i} |E_i| |E_j| ((\hat{G}_{ij}^* - G_{ij}) \cos \delta_{ij}(h) \\ & \left. + (\hat{B}_{ij}^* - B_{ij}) \sin \delta_{ij}(h)) \right) + \left(1 - \frac{d_i \tau}{m_i} + \lambda_i \right)^k \epsilon_i(0) \end{aligned} \quad (23)$$

Now, the following theorem is given to characterize such fault that can be detected by the proposed local fault detection logic.

Theorem 1 (Fault Detectability). Consider the adaptive threshold in (18) and the local fault detection logic. A fault s can be detected by the i th diagnosis component, if for some discrete-time sequence $[k_1, k_2]$ where $k_2 > k_1 > K_0$, such that the mismatch function $\chi_i(\delta_i(k), z_i(k))$ satisfies:

$$\begin{aligned} & \left| \sum_{h=k_1}^{k_2-1} \left(1 - \frac{d_i \tau}{m_i} + \lambda_i\right)^{k_2-1-k_1-h} \chi_i(\delta_i(h), z_i(h)) \right| > \\ & 2 \sum_{h=0}^{k_2-1} \left(1 - \frac{d_i \tau}{m_i} + \lambda_i\right)^{k_2-1-h} \left(\|H_i^T(h)\| \kappa_i(h) + \right. \\ & \quad \left. + \bar{\eta}_i(\delta_i(h), \omega_i(h), P_{mi}(h), h) + K_{\hat{g}} \|col(\delta_i(h), z_i(h))\| \right. \\ & \quad \left. + \left| \frac{\tau}{m_i} \sum_{j \in \mathcal{N}_i} |E_i| |E_j| (G_{ij} \cos \delta_{ij}(h) + B_{ij} \sin \delta_{ij}(h)) \right| \right) \\ & \quad + 2 \left(1 - \frac{d_i \tau}{m_i} + \lambda_i\right)^{k_2} |\epsilon_i(0)| \end{aligned} \quad (24)$$

Proof. Applying triangle inequality to (23), we have

$$\begin{aligned} |\epsilon_i(k)| & \geq \sum_{h=0}^{k-1} \left(1 - \frac{d_i \tau}{m_i} + \lambda_i\right)^{k-1-h} \left(|\chi_i(\delta_i(h), z_i(h))| \right. \\ & \quad \left. - \|H_i^T(h)\| \kappa_i(h) - \tau \bar{\eta}_i(\delta_i(h), \omega_i(h), P_{mi}(h), h) \right. \\ & \quad \left. - \left| \frac{\tau}{m_i} \sum_{j \in \mathcal{N}_i} |E_i| |E_j| ((\hat{G}_{ij}^* - G_{ij}) \cos \delta_{ij}(h) \right. \right. \\ & \quad \left. \left. + (\hat{B}_{ij}^* - B_{ij}) \sin \delta_{ij}(h)) \right| \right) - \left(1 - \frac{d_i \tau}{m_i} + \lambda_i\right)^k |\epsilon_i(0)| \end{aligned} \quad (25)$$

Notice the description of parameter estimate property and bounded interconnected function in (17), the above inequality becomes:

$$\begin{aligned} |\epsilon_i(k)| & \geq \sum_{h=0}^{k-1} \left(1 - \frac{d_i \tau}{m_i} + \lambda_i\right)^{k-1-h} \left(|\chi_i(\delta_i(h), z_i(h))| \right. \\ & \quad \left. - \|H_i^T(h)\| \kappa_i(h) - \tau \bar{\eta}_i(\delta_i(h), \omega_i(h), P_{mi}(h), h) \right. \\ & \quad \left. - K_{\hat{g}} \|col(\delta_i(k), z_i(k))\| \right. \\ & \quad \left. - \left| \frac{\tau}{m_i} \sum_{j \in \mathcal{N}_i} |E_i| |E_j| (G_{ij} \cos \delta_{ij}(h) + B_{ij} \sin \delta_{ij}(h)) \right| \right) \\ & \quad - \left(1 - \frac{d_i \tau}{m_i} + \lambda_i\right)^k |\epsilon_i(0)| \end{aligned} \quad (26)$$

According to the local fault detection logic, for $k_2 > K_0$, a fault is detected at time t_{k_2} with the residual-threshold

checking: $|\epsilon_i(k_2)| > \bar{\epsilon}_i(k_2)$, which is guaranteed by:

$$\begin{aligned} & \left| \sum_{h=0}^{k_2-1} \left(1 - \frac{d_i \tau}{m_i} + \lambda_i\right)^{k_2-1-h} \chi_i(\delta_i(h), z_i(h)) \right| > \\ & 2 \sum_{h=0}^{k_2-1} \left(1 - \frac{d_i \tau}{m_i} + \lambda_i\right)^{k_2-1-h} \left(\|H_i^T(h)\| \kappa_i(h) \right. \\ & \quad \left. + \tau \bar{\eta}_i(\delta_i(h), \omega_i(h), P_{mi}(h), h) + K_{\hat{g}} \|col(\delta_i(h), z_i(h))\| \right. \\ & \quad \left. + \left| \frac{\tau}{m_i} \sum_{j \in \mathcal{N}_i} |E_i| |E_j| (G_{ij} \cos \delta_{ij}(h) + B_{ij} \sin \delta_{ij}(h)) \right| \right) \\ & \quad + 2 \left(1 - \frac{d_i \tau}{m_i} + \lambda_i\right)^{k_2} |\epsilon_i(0)| \end{aligned} \quad (27)$$

while the fault detectability in (24) is a sufficient condition for the above inequality for $k_2 > k_1 > K_0$. The proof is completed. \square

C. Distributed Fault Isolation Scheme

Fault isolating by diagnosis agent i is achieved by a group of FIEs. Consider a known global fault set $\mathcal{M} = \{\phi_1, \phi_2, \dots, \phi_M\}$. Each fault $\phi_f \in \mathcal{M}$ leads to the changed admittance matrix \mathbf{Y}^f and interconnection power flow dynamics ΔP_{ij} . Now we introduce the following definitions to describe the relationships between faults and each diagnosis component.

Definition 2. For the fault $l \in \mathcal{M}$, its influence set \mathcal{I}_l is the set $\mathcal{I}_l \triangleq \{i | i \in \mathcal{V}_g, |\epsilon_i(k)| > \bar{\epsilon}_i(k)\}$.

Definition 3. For each diagnosis agent based on subsystem $i \in \mathcal{V}_g$, its local fault set \mathcal{M}_i is the set $\mathcal{M}_i \triangleq \{l | l \in \mathcal{M}, i \in \mathcal{I}_l\}$.

Remark. The fault influence set is obtained by running a fault detection simulation. Diagnosis agents satisfying the proposed fault detection logic will be included in a certain fault influence set.

FIE is constructed with an approximator storing certain fault information. Similar to the structure of FDAE in (8), a FIE r ($r \in \mathcal{M}_i$) is designed as

$$\begin{aligned} \hat{\delta}_{i,r}(k+1) &= \hat{\delta}_{i,r}(k) + \tau \hat{\omega}_{i,r}(k) \\ \hat{\omega}_{i,r}(k+1) &= \left(1 - \frac{d_i \tau}{m_i}\right) \hat{\omega}_{i,r}(k) + \frac{\tau}{m_i} P_{mi}(k) \\ & \quad + \hat{\phi}_{i,r}(\delta_i(k), z_i(k); \hat{\theta}_{i,r}) + \lambda_i (\hat{\omega}_{i,r}(k) - \omega_i(k)) \end{aligned} \quad (28)$$

where $0 < \lambda_i < 1$ is a design constant to adjust estimation degree, $\hat{\omega}_{i,r}$ is the estimate of state ω_i of FIE r . $\hat{\phi}_i(\delta_i, z_i; \hat{\theta}_{i,r})$ is the online approximation model designed to learn the unknown faulty interconnection function $g_i(\delta_i, z_i) + \phi_i(\delta_i, z_i)$, while $\hat{\theta}_{i,r}$ is a vector of adjustable parameters:

$$\begin{aligned} \hat{\phi}_i(\delta_i(k), z_i(k); \hat{\theta}_{i,r}) &:= -\frac{\tau}{m_i} \sum_{j \in \mathcal{N}_i} |E_i| |E_j| \hat{G}_{ij}^r \cos \delta_{ij}(k) \\ & \quad + |E_i| |E_j| \hat{B}_{ij}^r \sin \delta_{ij}(k) \\ \hat{\theta}_{i,r} &:= (\hat{G}_{ij}^r, \hat{B}_{ij}^r)^T \\ \hat{G}_{ij}^r &= col(\hat{G}_{ij}^r, j \in \mathcal{N}_i) \\ \hat{B}_{ij}^r &= col(\hat{B}_{ij}^r, j \in \mathcal{N}_i) \end{aligned} \quad (29)$$

Analogously to (10), the estimate parameter is updated according to the adaptive law:

$$\hat{\theta}_{i,r}(k+1) = \mathcal{P}(\hat{\theta}_{i,r}(k) + \gamma_{i,r}(k)H_{i,r}^T(k)\sigma_{i,r}(k+1)) \quad (30)$$

where $\sigma_r(k+1) = \epsilon_{i,r}(k+1) - \epsilon_{i,r}(k)$, $H_{i,r} \triangleq \partial \phi_i(\delta_i(k), z_i(k); \hat{\theta}_{i,r}) / \partial \hat{\theta}_{i,r}$, and $\mathcal{P}_{\hat{\theta}_{i,r}}$ is a suitable projection operator

$$\mathcal{P}_{\hat{\theta}_{i,r}}(\hat{\theta}_{i,r}) \triangleq \begin{cases} \hat{\theta}_{i,r}, & \text{if } |\hat{\theta}_i| \leq M_{\hat{\theta}_{i,r}} \\ \frac{M_{\hat{\theta}_{i,r}} \hat{\theta}_{i,r}}{|\hat{\theta}_i|}, & \text{if } |\hat{\theta}_i| > M_{\hat{\theta}_{i,r}} \end{cases} \quad (31)$$

The learning rate $\gamma_{i,r}(k)$ is computed at each step as $\gamma_{i,r}(t_k) \triangleq \mu_{i,r} / (\varepsilon_{i,r} + \|H_{i,r}^T(k)\|_F^2)$ with design constant $\varepsilon_{i,r} > 0$, $0 < \mu_{i,r} < 2$.

Now we assume that a fault $l \in \mathcal{M}$, is detected by diagnosis agent i , subsequently the group of FIEs is activated to monitor current faulty system. The state estimate error is

$$\begin{aligned} \epsilon_{i,r}(k) = & \sum_{h=K_d}^{k-1} \left(1 - \frac{d_i \tau}{m_i} + \lambda_i \right)^{k-1-K_d-h} \left(H_{i,r}^T(h) \tilde{\theta}_{i,r}(h) \right. \\ & - \tau \eta_i(\delta_i(h), \omega_i(h), P_{mi}(h), h) \\ & - \frac{\tau}{m_i} \sum_{j \in \mathcal{N}_i} |E_i| |E_j| ((\hat{G}_{ij}^{*r} - G_{ij}^l) \cos \delta_{ij}(h) \\ & \left. + (\hat{B}_{ij}^{*r} - B_{ij}^l) \sin \delta_{ij}(h)) \right) \\ & + (1 - \frac{d_i \tau}{m_i} + \lambda_i)^{k-K_d} \epsilon_i(K_d) \end{aligned} \quad (32)$$

where $\tilde{\theta}_{i,r} \triangleq \hat{\theta}_{i,r} - \hat{\theta}_{i,r}^*$.

Applying triangle inequality:

$$\begin{aligned} |\epsilon_{i,r}(k)| \leq & \sum_{h=K_d}^{k-1} \left(1 - \frac{d_i \tau}{m_i} + \lambda_i \right)^{k-1-K_d-h} \left(\|H_{i,r}^T(h)\| \kappa_{i,r}(h) \right. \\ & + \tau \bar{\eta}_i(\delta_i(h), \omega_i(h), P_{mi}(h), h) \\ & + \left| \frac{\tau}{m_i} \sum_{j \in \mathcal{N}_i} |E_i| |E_j| ((\hat{G}_{ij}^{*r} - G_{ij}^l) \cos \delta_{ij}(h) \right. \\ & \left. + (\hat{B}_{ij}^{*r} - B_{ij}^l) \sin \delta_{ij}(h)) \right| \\ & \left. + (1 - \frac{d_i \tau}{m_i} + \lambda_i)^{k-K_d} |\epsilon_i(K_d)| \right) \end{aligned} \quad (33)$$

Considering that the FIE r matches the fault l , that is $r = l$. Thus $\hat{\theta}_{i,r}^*$ is able to approximate $\theta_{i,l}$ in a bounded region, that is $|\hat{\theta}_{i,r}^* - \theta_{i,l}| = |\hat{\theta}_{i,r}^* - \theta_{i,r}| \leq \bar{\theta}_{i,r}^*$, where $\bar{\theta}_{i,r}^* = (\bar{G}_{ij}^{*r}, \bar{B}_{ij}^{*r})$. The above inequality becomes:

$$\begin{aligned} |\epsilon_{i,r}(k)| \leq & \sum_{h=K_d}^{k-1} \left(1 - \frac{d_i \tau}{m_i} + \lambda_i \right)^{k-1-K_d-h} \left(\|H_{i,r}^T(h)\| \kappa_{i,r}(h) \right. \\ & + \tau \bar{\eta}_i(\delta_i(h), \omega_i(h), P_{mi}(h), h) \\ & + \frac{\tau}{m_i} \sum_{j \in \mathcal{N}_i} |E_i| |E_j| ((\bar{G}_{ij}^{*r} + \bar{B}_{ij}^{*r})) \\ & \left. + (1 - \frac{d_i \tau}{m_i} + \lambda_i)^{k-K_d} |\epsilon_i(K_d)| \right) \triangleq \bar{\mu}_{i,r}(k) \end{aligned} \quad (34)$$

where $\bar{\mu}_{i,r}(k)$ is the adaptive threshold designed for FIE r .

Consider FIE r doesn't match fault l , that is $r \neq l$. See (33), the parameter bias $\hat{\theta}_{i,r}^* - \theta_{i,l}$ may result in a large fluctuation so that $|\epsilon_{i,r}(k)| > \bar{\mu}_{i,r}(k)$. Analogously, *mismatch function* is introduced to describe the bias between two types of faults:

$$\chi_i^{r,l}(k) \triangleq -\frac{\tau}{m_i} \sum_{j \in \mathcal{N}_i} |E_i| |E_j| (\Delta G_{ij}^{r,l} \cos \delta_{ij}(k) + \Delta B_{ij}^{r,l} \sin \delta_{ij}(k)) \quad (35)$$

where $\Delta G_{ij}^{r,l} = G_{ij}^r - G_{ij}^l$, $\Delta B_{ij}^{r,l} = B_{ij}^r - B_{ij}^l$ are *non-matched parameter bias*, that is $\Delta \theta_i^{r,l} := (\Delta G_{ij}^{r,l}, \Delta B_{ij}^{r,l})$.

Proposition 2 (Local fault isolation logic). A fault l is isolated by diagnosis agent i , if, for each $r \in \mathcal{M}_i \setminus \{l\}$, there exist some finite discrete-time instant $t^r > T_d$ such that $|\epsilon_{i,r}(t^r)| > \bar{\mu}_{i,r}(t^r)$, then the occurrence of fault l is deduced. The absolute fault isolation time is defined as

$$T_{isol}^s \triangleq \max\{t^r, r \in \mathcal{M}_i \setminus \{s\}\} \quad (36)$$

and the fault isolation time t_{isol}^s is defined as the difference between T_{isol}^s and the absolute fault detection time T_d , i.e., $t_{isol}^s \triangleq T_{isol}^s - T_d$.

D. Fault Isolability Analysis

Theorem 2 (Fault isolability). Given a fault $l \in \mathcal{M}$, if for each $r \in \mathcal{O}_i \setminus \{l\}$, there exists some discrete-time instant $k^r > K_d$, such that

$$\begin{aligned} & \left| \sum_{h=K_d}^{k^r-1} \lambda_i^{k^r-1-K_d-h} \chi_i^{r,l}(h) \right| > \\ & 2 \sum_{h=K_d}^{k^r-1} \left(1 - \frac{d_i \tau}{m_i} + \lambda_i \right)^{k^r-1-K_d-h} \left(\|H_{i,r}^T(h)\| \kappa_{i,r}(h) \right. \\ & + \tau \bar{\eta}_i(\delta_i(h), \omega_i(h), P_{mi}(h), h) \\ & + \frac{\tau}{m_i} \sum_{j \in \mathcal{N}_i} |E_i| |E_j| ((\bar{G}_{ij}^{*r} + \bar{B}_{ij}^{*r})) \\ & \left. + 2(1 - \frac{d_i \tau}{m_i} + \lambda_i)^{k^r-K_d} |\epsilon_i(K_d)| \right) \end{aligned} \quad (37)$$

then, the fault l can be isolated by group of FIEs.

Proof. Consider a FIE r , is monitoring the system at the occurrence of fault l , $r \neq l$. Using mismatch function in (35), the estimate error is

$$\begin{aligned} \epsilon_{i,r}(k) = & \sum_{h=K_0}^{k-1} \left(1 - \frac{d_i \tau}{m_i} + \lambda_i \right)^{k-1-K_d-h} \left(H_{i,r}^T(h) \tilde{\theta}_{i,r}(h) \right. \\ & - \tau \eta_i(\delta_i(h), \omega_i(h), P_{mi}(h), h) + \chi_i^{r,l}(h) \\ & - \frac{\tau}{m_i} \sum_{j \in \mathcal{N}_i} |E_i| |E_j| ((\hat{G}_{ij}^{*r} - G_{ij}^r) \cos \delta_{ij}(h) \\ & \left. + (\hat{B}_{ij}^{*r} - B_{ij}^r) \sin \delta_{ij}(h)) \right) \\ & + (1 - \frac{d_i \tau}{m_i} + \lambda_i)^{k-K_d} \epsilon_i(K_d) \end{aligned} \quad (38)$$

applying triangle inequality:

$$\begin{aligned}
|\epsilon_{i,r}(k)| \geq & \sum_{h=K_0}^{k-1} \left(1 - \frac{d_i \tau}{m_i} + \lambda_i\right)^{k-1-h} \left(\chi_i^{r,l}(h) \right. \\
& - \|H_{i,r}^T(h)\| \kappa_{i,r}(h) \\
& - \tau \bar{\eta}_i(\delta_i(h), \omega_i(h), P_{mi}(h), h) \\
& - \frac{\tau}{m_i} \sum_{j \in \mathcal{N}_i} |E_i| |E_j| (\bar{G}_{ij}^{*r} + \bar{B}_{ij}^{*r}) \\
& \left. - \left(1 - \frac{d_i \tau}{m_i} + \lambda_i\right)^{k-K_d} |\epsilon_i(K_d)| \right) \quad (39)
\end{aligned}$$

see the fault isolation threshold in (34), if the condition in (37) holds, then for some $k^r > K_d$,

$$|\epsilon_{i,r}(k^r)| > \bar{\mu}_{i,r}(k^r)$$

which shows that each FIE r ($r \in \mathcal{O}_i \setminus \{l\}$) has excluded fault l . Proof is completed. \square

IV. SIMULATION

In this section, we illustrate the effectiveness of the proposed distributed FDI method in the IEEE 9 and 39 bus power system. The admittance changes described in (3) is caused by the following fault sequence, which is similar to [5]:

Stage 1: The system is in a prefault steady state.

Stage 2: A symmetrical three-phase short circuit fault occurs near a certain bus, at $t = 0.5$ s.

Stage 3: The fault is removed by protectors of the faulted line at $t = 0.6$ s.

Stage 4: The system is in a postfault state.

The timely action of protection devices ensure the stability [28] and the system state ω_i bounded. Since the sampling frequency can be achieved as high as 2500Hz [31], the sampling period is set as 20ms in this simulation. Estimators have the following design parameters: $\lambda_i = 0.8$, $\varepsilon_i = 0.9$, $\mu_i = 1.8$. Moreover, 10% error for the initial parameter $\hat{\theta}_{i0}$ and 5% measurement noise are considered.

A. IEEE 9 bus 3 machine power system

The configuration of IEEE 9 bus system is given in Table I, with base MVA = 100. For each $\hat{\theta}_i$, we assume $0.8\hat{\theta}_{i0} < \hat{\theta}_i < 1.2\hat{\theta}_{i0}$, thus the geometric radius can be calculated: $\kappa_1 = 1.32$, $\kappa_2 = 1.47$, $\kappa_3 = 1.13$. In healthy condition, the system is in steady state, that is $\dot{\delta}_i = 0$, $\dot{\omega}_i = 0$. However, due to the modeling error $\Delta\hat{\theta}_{i0}$, the estimate state $col(\hat{\delta}_i, \hat{\omega}_i : i = 1, \dots, N)$ will probably get out of steady state without parameter adaption. A comparison of estimators with or without parameter adjustment is made, which is shown in Fig 1.

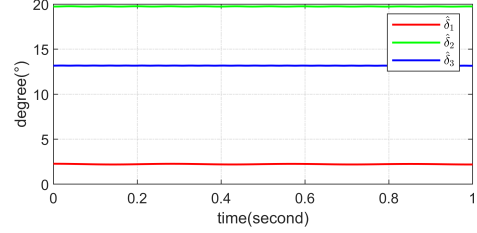
A global fault set $\mathcal{M} = \{1, 2, 3, 4, 5, 6\}$ and corresponding fault influence set are shown in Table II. As a relatively small power grid, all of the faults in \mathcal{M} are found to be detected by each local fault diagnosis agent in the simulations, thus $\mathcal{F}_1 = \mathcal{F}_2 = \mathcal{F}_3 = \{1, 2, 3, 4, 5, 6\}$.

Consider fault 2: symmetrical three-phase short circuit fault occurs in line 4-6, near bus 4. Fig 2 shows the time-behavior of each FDAE. During $t = 0 \sim 0.5$ s, system is in steady

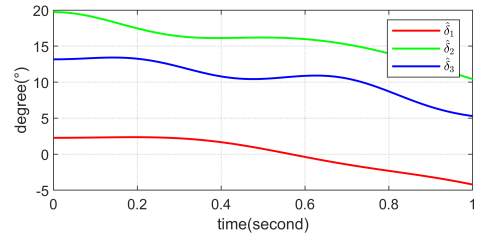
TABLE I
IEEE 9 BUS SYSTEM CONFIGURATION

node	$\delta_{i0} (^{\circ})$	$P_{mi0}(pu)$	d_i	$H_i(s)$	$E_i(pu)$
1	0.716	0.250	0	23.64	1.0566
2	1.630	0.576	0	6.4	1.0502
3	0.850	0.650	0	3.01	1.0170

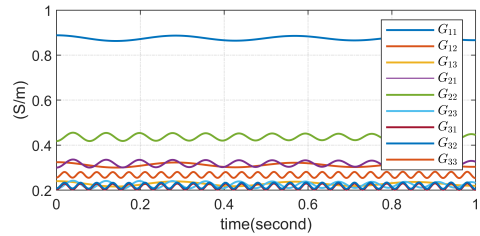
$m_i = 2H_i/120\pi$



(a) With parameter adaption, the estimate states remain steady.



(b) Without parameter adaption, the estimate states may get out of steady state.



(c) Parameter adaption in healthy condition.

Fig. 1. A comparison of two cases of estimators with and without parameter adaption in healthy condition.

TABLE II
FAULT VERSIONS OF IEEE 9 BUS SYSTEM

Fault	Position	Influence set
1	in line 4-5, near bus 4	1,2,3
2	in line 4-6, near bus 4	1,2,3
3	in line 5-7, near bus 5	1,2,3
4	in line 6-9, near bus 6	1,2,3
5	in line 7-8, near bus 7	1,2,3
6	in line 8-9, near bus 8	1,2,3

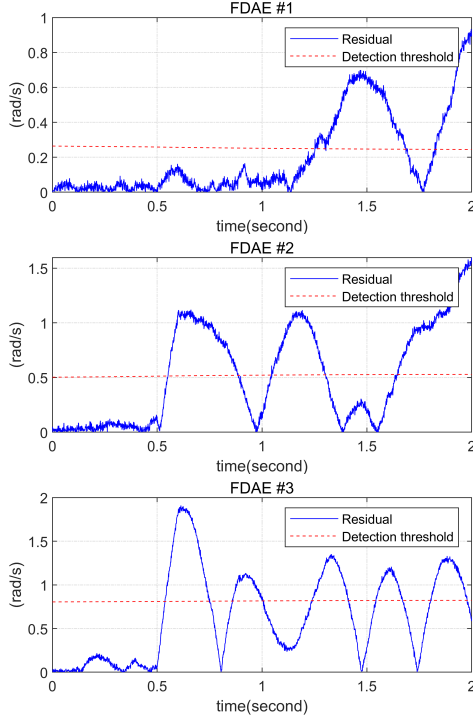


Fig. 2. A fault detection case: fault 2 occurred at $t = 0.5s$, and each FDAE announced ‘detected’ in few seconds.

state, and all the residuals do not exceed the thresholds. At $t = 0.5s$, fault 2 is introduced, and the system admittance parameters $col(G_{ij}, B_{ij} : i, j = 1, \dots, N)$ are totally changed. With the help of the projection operator (12), the parameters are limited to a known domain, leading to the surge of the residuals that ultimately exceeded the threshold, which means each local fault diagnosis agent has completed the detection assignment.

Subsequently, the groups of FIE are activated to monitor the faulty system. Focus on diagnosis agent 1 (marked as #1), where each FIE corresponds to a fault in \mathcal{F}_1 : FIE 1 to fault 1, FIE 2 to fault 2, ..., FIE 6 to fault 6. The time-behavior of each FIE is shown in Fig 3. We can see that each FIE except FIE 2 triggered the threshold checking, indicating the occurrence of fault 2.

B. IEEE 39 bus 10 machine power system

The configuration of IEEE 39 bus system is given in Table III, with base MVA = 1000. Using condition $G_{ij}^2 + B_{ij}^2 < 1$ to ignore some weak connections, the generator neighborhood sets are obtained: $\mathcal{N}_1 = \{1, 8, 9, 13\}$, $\mathcal{N}_2 = \{2, 3, 13\}$, $\mathcal{N}_3 = \{2, 3, 13\}$, $\mathcal{N}_4 = \{4, 5, 6, 7\}$, $\mathcal{N}_5 = \{4, 5\}$, $\mathcal{N}_6 = \{4, 6, 7\}$, $\mathcal{N}_7 = \{4, 6, 7\}$, $\mathcal{N}_8 = \{1, 8, 9\}$, $\mathcal{N}_9 = \{1, 8, 9\}$, $\mathcal{N}_{10} = \{10, 11, 13\}$, $\mathcal{N}_{11} = \{10, 11, 12, 13, 16\}$, $\mathcal{N}_{12} = \{11, 12, 13, 16\}$, $\mathcal{N}_{13} = \{1, 2, 3, 10, 11, 12, 13, 14, 16\}$, $\mathcal{N}_{14} = \{13, 14, 15\}$, $\mathcal{N}_{15} = \{14, 15, 16\}$, $\mathcal{N}_{16} = \{11, 12, 13, 15, 16\}$. For each θ_i , we assume $0.8\theta_{i0} < \theta_i < 1.2\theta_{i0}$, the geometric radius can be calculated : $\kappa_1 = 0.77$, $\kappa_2 = 0.19$, $\kappa_3 = 0.27$, $\kappa_4 = 0.72$, $\kappa_5 = 0.51$, $\kappa_6 = 0.31$, $\kappa_7 = 0.07$, $\kappa_8 = 0.67$, $\kappa_9 = 0.21$, $\kappa_{10} = 0.14$.

TABLE III
IEEE 39 BUS SYSTEM CONFIGURATION

node	$\delta_{i0} (^\circ)$	$P_{mi0} (pu)$	d_i	$H_i (s)$	$E_i (pu)$
30	-4.59	0.250	0	4.20	1.0475
31	0.00	0.576	0	3.03	0.9820
32	1.62	0.650	0	3.58	0.9831
33	2.06	0.632	0	2.86	0.9972
34	0.63	0.508	0	2.60	1.0123
35	4.04	0.650	0	2.64	1.0493
36	6.73	0.560	0	3.48	1.0635
37	1.14	0.540	0	2.43	1.0278
38	6.43	0.830	0	3.45	1.0265
39	-11.10	1.000	0	50.00	1.0300

$m_i = 2H_i/120\pi$.

TABLE IV
FAULT INFLUENCE SET OF IEEE 39 BUS SYSTEM

Fault	Position	Influence set
1	in line 1-2, near bus 1	1,2,3,9
2	in line 2-3, near bus 2	1,2,3,4,5,6,7,8,9,10
3	in line 3-4, near bus 3	1,2,3,4,5,6,7,8,9,10
4	in line 4-5, near bus 4	2,3,8,9
5	in line 5-6, near bus 5	2,3,9
6	in line 6-7, near bus 6	2,3,9
7	in line 7-8, near bus 7	2
8	in line 8-9, near bus 8	2,3,9
9	in line 10-11, near bus 10	2,3,9
10	in line 11-12, near bus 11	2,3
11	in line 13-14, near bus 13	2,3
12	in line 14-15, near bus 14	2,3,4,7,9,10
13	in line 15-16, near bus 15	2,3,4,5,6,7,9,10
14	in line 16-17, near bus 16	1,2,3,4,5,6,7,8,9,10
15	in line 17-18, near bus 17	1,2,3,4,5,6,7,8,9,10
16	in line 18-3, near bus 18	1,2,3,4,5,6,7,8,9,10
17	in line 21-22, near bus 21	4,5,6,7
18	in line 22-23, near bus 22	2,3,4,5,6,7
19	in line 23-24, near bus 23	4,5,6,7
20	in line 24-16, near bus 24	4,5,6,7
21	in line 25-26, near bus 25	1,2,3,4,5,6,7,8,9,10
22	in line 26-27, near bus 26	1,2,3,4,5,6,7,8,9,10
23	in line 27-17, near bus 27	1,2,3,7,9,10
24	in line 28-29, near bus 28	1,2,3,4,5,6,7,9,10

A global fault set $\mathcal{M} = \{1, 2, \dots, 24\}$ and corresponding fault influence set are shown in Table IV. It can be shown that, as the scale of the grid increases, a fault is hard to be detected by all diagnosis agent. The local fault set of each diagnosis agent is shown in Table V.

Consider fault 4: symmetrical three-phase short circuit fault occurs in line 4-5, near bus 4. The time-behaviour of each FDAE is shown in Fig 4 After the introduction of fault at $t = 0.5s$, diagnosis agent $\{2, 3, 8, 9\}$ detect the occurrence of

TABLE V
LOCAL FAULT SETS OF IEEE 39 BUS SYSTEM

Local fault set	Fault
\mathcal{F}_1	1,2,3,14,15,16,21,22,23,24
\mathcal{F}_2	1,2,3,4,5,6,7,8,9,10,11,12,13,14,15,16,18,21,22,23,24
\mathcal{F}_3	1,2,3,4,5,6,8,9,10,11,12,13,14,15,16,18,21,22,23,24
\mathcal{F}_4	2,3,13,14,15,16,17,18,19,20,21,22,24
\mathcal{F}_5	2,3,12,13,14,15,16,17,18,19,20,21,22,24
\mathcal{F}_6	2,3,13,14,15,16,17,18,19,20,21,22,24
\mathcal{F}_7	2,3,12,13,14,15,16,17,18,19,20,21,22,23,24
\mathcal{F}_8	2,3,4,14,15,16,17,22
\mathcal{F}_9	1,2,3,4,5,6,8,9,12,13,14,15,16,21,22,23,24
\mathcal{F}_{10}	2,3,12,13,14,15,16,21,22,23,24

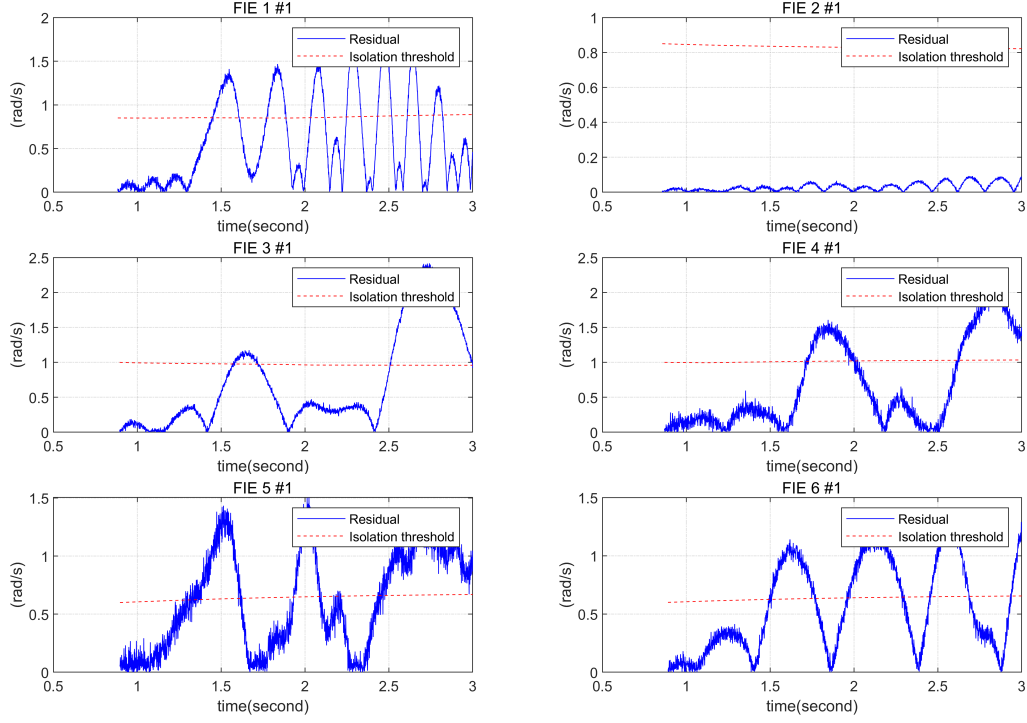


Fig. 3. A case of fault isolation for diagnosis agent 1: fault 2 occurred at $t = 0.5s$. All FIEs except FIE 2 triggered the threshold decision logic within a limited time, indicating the occurrence of fault 2.

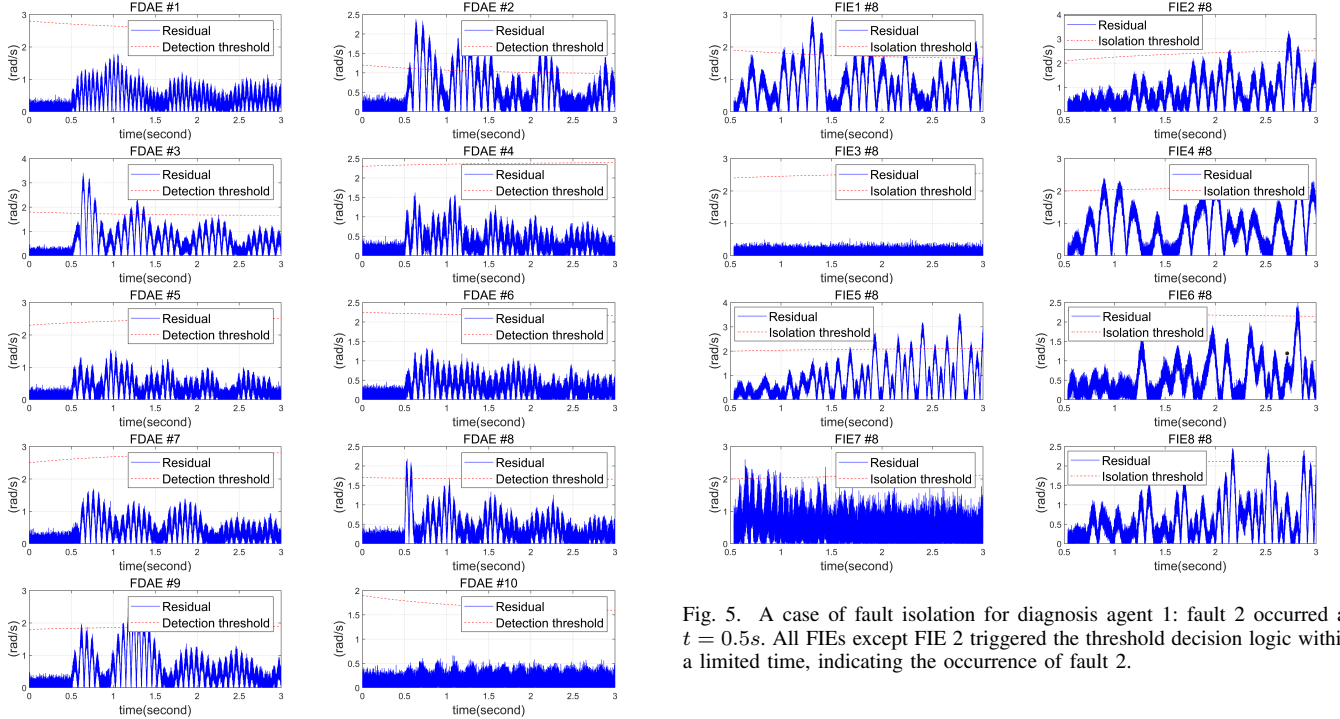


Fig. 4. A case of fault isolation of 9 bus system by diagnosis agent 1: fault 2 occurred at $t = 0.5s$. All FIEs except FIE 2 triggered the threshold decision logic within a limited time, indicating the occurrence of fault 2.

fault.

V. CONCLUSIONS

In this paper, a distributed fault detection and isolation scheme for multimachine power systems is proposed. The design of the proposed scheme contains: constructing fault detection and approximation estimators (FDAE); constructing fault isolation estimators (FIE); generating residuals and corresponding thresholds; analysing fault detectability and

isolability. The proposed fault detection and isolation scheme has the following characteristics:

- Only generators buses are required to deploy PMU;
- Parameter adaption increase the robustness to parameter modeling uncertainty;
- Distributed scheme improve the reliability of the diagnosis system since a fault can be detected or isolated by more than one diagnosis components.
- The complement of different diagnosis components overcome the local fault detectability and isolability problem.

In future work, we hope to integrate sensor and actuator faults into an entire framework. In addition, the design of fault-tolerant systems based on power systems dynamic model is also an attractive topic.

REFERENCES

- [1] M. Shahidehpour, F. Tinney, and Y. Fu, "Impact of security on power systems operation," *Proceedings of the IEEE*, vol. 93, no. 11, pp. 2013–2025, 2005.
- [2] J. Weimer, S. Kar, and K. H. Johansson, "Distributed detection and isolation of topology attacks in power networks," in *Proceedings of the 1st international conference on High Confidence Networked Systems*. ACM, 2012, pp. 65–72.
- [3] W. Pan, Y. Yuan, H. Sandberg, J. Gonçalves, and G.-B. Stan, "Online fault diagnosis for nonlinear power systems," *Automatica*, vol. 55, pp. 27–36, 2015.
- [4] Q. Zhang and X. Zhang, "Distributed fault detection and isolation for multimachine power systems," in *Proceedings of 2012 IEEE/ASME 8th IEEE/ASME International Conference on Mechatronic and Embedded Systems and Applications*. IEEE, 2012, pp. 241–246.
- [5] T. Chen, D. J. Hill, and C. Wang, "Distributed fast fault diagnosis for multimachine power systems via deterministic learning," *IEEE Transactions on Industrial Electronics*, 2019.
- [6] Q. Zhang, X. Zhang, M. M. Polycarpou, and T. Parisini, "Distributed sensor fault detection and isolation for multimachine power systems," *International Journal of Robust and Nonlinear Control*, vol. 24, no. 8–9, pp. 1403–1430, 2014.
- [7] M. Pignati, L. Zanni, P. Romano, R. Cherkaoui, and M. Paolone, "Fault detection and faulted line identification in active distribution networks using synchrophasors-based real-time state estimation," *IEEE Transactions on Power Delivery*, vol. 32, no. 1, pp. 381–392, 2016.
- [8] F. Chowdhury, J. P. Christensen, and J. L. Aravena, "Power system fault detection and state estimation using kalman filter with hypothesis testing," *IEEE transactions on Power Delivery*, vol. 6, no. 3, pp. 1025–1030, 1991.
- [9] M. Karthikeyan and V. Malathi, "Wavelet-support vector machine approach for classification of power quality disturbances," *International Journal of Recent Trends in Engineering*, vol. 1, no. 3, p. 290, 2009.
- [10] A. M. Elhaffar *et al.*, "Power transmission line fault location based on current traveling waves," 2008.
- [11] D. Das, N. K. Singh, and A. K. Sinha, "A comparison of fourier transform and wavelet transform methods for detection and classification of faults on transmission lines," in *2006 IEEE Power India Conference*. IEEE, 2006, pp. 7–pp.
- [12] K. Li, L. Lai, and A. David, "Application of artificial neural network in fault location technique," in *DRPT2000. International Conference on Electric Utility Deregulation and Restructuring and Power Technologies. Proceedings (Cat. No. 00EX382)*. IEEE, 2000, pp. 226–231.
- [13] E. Vazquez, H. J. Altuve, and O. L. Chacon, "Neural network approach to fault detection in electric power systems," in *Proceedings of International Conference on Neural Networks (ICNN'96)*, vol. 4. IEEE, 1996, pp. 2090–2095.
- [14] M. Uyar, S. Yildirim, and M. T. Gencoglu, "An effective wavelet-based feature extraction method for classification of power quality disturbance signals," *Electric power systems Research*, vol. 78, no. 10, pp. 1747–1755, 2008.
- [15] J. Zhao, Y. Xu, F. Luo, Z. Dong, and Y. Peng, "Power system fault diagnosis based on history driven differential evolution and stochastic time domain simulation," *Information Sciences*, vol. 275, pp. 13–29, 2014.
- [16] S. Ekici, S. Yildirim, and M. Poyraz, "Energy and entropy-based feature extraction for locating fault on transmission lines by using neural network and wavelet packet decomposition," *Expert Systems with Applications*, vol. 34, no. 4, pp. 2937–2944, 2008.
- [17] P. Jafarian and M. Sanaye-Pasand, "High-frequency transients-based protection of multiterminal transmission lines using the svm technique," *IEEE Transactions On Power Delivery*, vol. 28, no. 1, pp. 188–196, 2012.
- [18] S. Kalyani and K. S. Swarup, "Binary svm approach for security assessment and classification in power systems," in *2009 Annual IEEE India Conference*. IEEE, 2009, pp. 1–4.
- [19] I. Farhat, "Fault detection, classification and location in transmission line systems using neural networks," Ph.D. dissertation, Concordia University, 2003.
- [20] P. L. Mao and R. K. Aggarwal, "A novel approach to the classification of the transient phenomena in power transformers using combined wavelet transform and neural network," *IEEE Transactions on Power Delivery*, vol. 16, no. 4, pp. 654–660, 2001.
- [21] R. Aggarwal and Y. Song, "Artificial neural networks in power systems. part 1: General introduction to neural computing," *Power Engineering Journal*, vol. 11, no. 3, pp. 129–134, 1997.

- [22] I. Shames, A. M. Teixeira, H. Sandberg, and K. H. Johansson, "Distributed fault detection for interconnected second-order systems," *Automatica*, vol. 47, no. 12, pp. 2757–2764, 2011.
- [23] R. M. Ferrari, T. Parisini, and M. M. Polycarpou, "A fault detection scheme for distributed nonlinear uncertain systems," in *2006 IEEE Conference on Computer Aided Control System Design, 2006 IEEE International Conference on Control Applications, 2006 IEEE International Symposium on Intelligent Control*. IEEE, 2006, pp. 2742–2747.
- [24] —, "Distributed fault detection and isolation of large-scale discrete-time nonlinear systems: An adaptive approximation approach," *IEEE Transactions on Automatic Control*, vol. 57, no. 2, pp. 275–290, 2011.
- [25] X. Zhang, M. M. Polycarpou, and T. Parisini, "A robust detection and isolation scheme for abrupt and incipient faults in nonlinear systems," *IEEE transactions on automatic control*, vol. 47, no. 4, pp. 576–593, 2002.
- [26] V. Reppa, M. M. Polycarpou, and C. G. Panayiotou, "Distributed sensor fault diagnosis for a network of interconnected cyberphysical systems," *IEEE Transactions on Control of Network Systems*, vol. 2, no. 1, pp. 11–23, 2014.
- [27] P. M. Anderson and A. A. Fouad, *Power system control and stability*. John Wiley & Sons, 2008.
- [28] P. Kundur, N. J. Balu, and M. G. Lauby, *Power system stability and control*. McGraw-hill New York, 1994, vol. 7.
- [29] C. Liu, B. Wang, and K. Sun, "Fast power system dynamic simulation using continued fractions," *IEEE Access*, vol. 6, no. 99, pp. 62 687–62 698, 2018.
- [30] R. M. Ferrari, T. Parisini, and M. M. Polycarpou, "A fault detection and isolation scheme for nonlinear uncertain discrete-time systems," in *2007 46th IEEE Conference on Decision and Control*. IEEE, 2007, pp. 1009–1014.
- [31] J. E. Tate and T. J. Overbye, "Line outage detection using phasor angle measurements," *IEEE Transactions on Power Systems*, vol. 23, no. 4, pp. 1644–1652, 2008.